■ Original Article ■

Functionalizing Liposomes with Dual Aptamers for Targeting of Breast Cancer Cells and Cancer Stem Cells

Hee-Bin Park[§,*], Ji-Eun You[§,*], Pyung-Hwan Kim[**] and Keun-Sik Kim[†,**]

Department of Biomedical Laboratory Science, Konyang University, Daejeon 35365, Korea

Cancer stem cells, which are known to drive tumor formation and maintenance, are a major obstacle in the effective treatment of various types of cancer. Trans-membrane glycoprotein mucin 1 antigen and cell surface glycogen CD44 antigen are well-known surface markers of breast cancer cells and breast cancer stem cells, respectively. To effectively treat cancer cells and cancer stem cells, we developed a new drug-encapsulating liposome conjugated with dual-DNA aptamers specific to the surface markers of breast cancer cells and their cancer stem cells. These two aptamer (Apt)-targeted liposomes, which were prepared to encapsulate doxorubicin (Dox), were named "Dual-Apt-Dox". Dual-Apt-Dox is significantly more cytotoxic to both cancer stem cells and cancer cells compared to liposomes lacking the aptamers. Furthermore, we demonstrated the inhibitory efficacy of Dual-Apt-Dox against the experimental lung metastasis of breast cancer stem cells and cancer cells in athymic nude mice. We also showed the potent antitumor effects of dual-aptamer-conjugated liposome systems by targeting cancer cells as well as cancer stem cells. Thus, our data indicate that dual-aptamer-conjugated liposome systems can prove to be effective drug delivery vehicles for breast cancer therapy.

Key Words: Aptamer, Cancer stem cells, Chemotherapy, Drug delivery, Liposomes

INTRODUCTION

Breast cancer is the most frequent cancer (Comşa et al., 2015) and is expected to account for 29% of all cancer cases and 14% of cancer deaths (Siegel et al., 2016). Over the past decades, an improved survival rate and early diagnosis have improved breast cancer mortality statistics (Crabtree and Miele, 2018). However, because of these invasive features (the recurrence and metastasis of breast cancer cells), the treatment of breast cancer cells remains a challenge (Lin et al., 2012b). The underlying presence of breast cancer cells, regarded as breast cancer stem cells (BCSCs) with an ele-vated expression of CD44 cell surface markers (Sin and Lim, 2017) and lack of expression of CD24 (CD44+/CD24-), most likely drives progression or metastasis (Lin et al., 2012b). Cancer stem cells (CSCs) are resistant to the anti-cancer effects of routine chemotherapy and radiotherapy (Sheridan et al., 2006) and appear to be an important barrier to the successful treatment of breast cancer (Fan et al., 2017).

Doxorubicin (Dox) is one of the most widely used drugs for the treatment of breast cancer in adjuvant settings as well as in patients with metastatic disease (Yan et al., 2017). In addition, Dox treatment during the initial and metastatic stages of breast cancer may delay or stop the growth of cancer cells (Trebunova et al., 2012). Recent studies have

shown that Dox induces toxicity to reduce the chemo-resistance of CSCs and induces cell death (Yan et al., 2017). However, Dox has been shown to accumulate in the heart, potentially leading to congestive heart failure, which limits its therapeutic use (Yi et al., 2010). Therefore, it is necessary to develop a drug delivery system capable of reducing toxicity to normal cells and targeting only cancer cells and CSCs.

To overcome the limitations of conventional drug delivery systems, nanocarriers that can effectively deliver drugs are being developed (Patra et al., 2018). Among the various nanocarrier types currently being studied, liposomes are considered one of the most promising systems for drug delivery (Khodabandehloo et al., 2016). Due to their unique structure, liposomes can capture hydrophobic materials in lipid bilayers (Xing et al., 2016) and encapsulate hydrophilic materials inside the central aqueous areas to prevent agent degradation (Li et al., 2015). However, when administered intravenously, liposomes are rapidly absorbed by the reticuloendothelial system (RES) of the liver and spleen (Group, 2002). This phenomenon prevents their long-term circulation in the blood and reduces the efficiency of targeting tumor tissue when liposomes are administered into the drug delivery system (Ghannam et al., 2016). To circumvent this problem, liposomes can be chemically modified by attaching polyethylene glycol (PEG) for increased stability (Pasut et al., 2015).

Liposomes can be conjugated to various target ligands, such as peptides, aptamers, and antibody fragments, using targeted engineering techniques to develop targeted liposomes (Saw et al., 2015). Nucleic acid aptamers are small single-stranded DNA or RNA oligonucleotides (usually spanning 25~90 nucleosides) (Guan et al., 2018). Based on a unique three-dimensional structure, nucleic acid aptamers specifically bind to target molecules with high specificity and binding affinities (Bayrac et al., 2011). Aptamers also have characterized by their non-immunogenicity, rapid tissue penetration, and stability at high temperatures compared to other ligands such as antibodies or peptides (Kim et al., 2018).

In this study, MUC-1 and CD44 aptamers were used to target breast cancer cells and BCSCs, respectively. A novel targeted nanocarrier system was developed by conjugating two aptamers to liposomes and was named "dual-aptamosome".

In addition, Dox, an anticancer drug, was delivered via dual-aptamosomes (Dual-Apt-Dox). We confirmed that the Dual-Apt-Dox system has excellent therapeutic effects *in vitro* and *in vivo*, without the limitations of conventional chemotherapeutic agents, such as instability, short half-life, and off-target effect.

MATERIALS AND METHODS

Cell Culture

MCF-7 and HepG2 cells were purchased from the American Types Culture Collection (ATCC, Manassas, VA, USA). MCF-7 and HepG2 cells were maintained in Eagle's Minimum Essential Medium (EMEM) (ATCC, Manassas, VA, USA) supplemented with 10% heat-inactivated fetal bovine serum (FBS) and 1% penicillin and streptomycin (GE healthcare, Chicago, IL, USA). MCF-7 cells and HepG2 cells were cultured in an incubator in 5% CO_2 at 37℃.

Breast cancer stem cell culture and isolation

Breast cancer stem cell were isolated from MCF-7. The MCF-7 cells (2×10^4 cells/well) were seeded on 6-well ultralow adherence plates (Corning, NY, USA) in DMEM/F-12 (Gibco, USA) including 5 mg/mL insulin, 2% B27 (Invitrogen Ltd., Paisley, Scotland), 20 ng/mL epidermal growth factor (EGF), 20 ng/mL basic fibroblast growth factor (bFGF) (both from Peprotech, USA) and were poured into plates 2 mL per well. In this condition, MCF-7 cells were cultured 14 days and passaged every 7 days. The features of MCF-7 cells disappeared, and the characteristic of CSCs increased, and cells formed mammospheres. BCSCs were harvested and washed in PBS by centrifugation at 1,000 rpm for 3 min. After centrifugation, the harvested cells were suspended with trypsin and then neutralized in serum-free DMEM/F12 medium at a 1:1 ratio and dissociated by pipetting with a 23-gauge needle. After confirming for single cells, the cells were plated in DMEM/F12 medium to 20,000 cells per well in ultralow adherence plates. After 2 weeks of incubation, BCSCs were collected to isolate the CD44+ CD24-/low phenotype in BCSCs and I conducted according to the manufacturer's instructions for the human CD44+/CD24- breast cancer stem cell isolation kit (R&D system,

Minneapolis, MN, USA).

Cell specific binding observation of MUC-1/CD44 aptamer

Specific cellular binding affinities of MUC-1/CD44 aptamer were observed in MCF-7 cells and BCSCs with a Axio Zeiss A1 Imager compound microscope (CarlZeiss, Oberkochen, Germany). The MCF-7 cells (2×10^4 cells/well) and BCSCs (2×10^4 cells/well) were grown in 24 well plate for 24 hrs. Cells were washed twice with PBS and fixed with 4% paraformaldehyde (*w/v*) for 30 min at room temperature. Then cells were treated with MUC-1/CD44 aptamers at room temperature for 1 hr. After incubation, the cells were washed with PBS and mounted. Cells were observed with an Axio Zeiss A1 Imager microscope.

Preparation micelle and doxorubicin-encapsulation liposome

To make micells DSPE-PEG$_{2000}$ and DSPE-PEG$_{2000}$-Mal were mixed at a molar ratio of 1:4 in chloroform:metanol (2:1, *v/v*) by nitrogen gas. PEG-DSPE-$_{2000}$, POPC and Cholesterol (0.1:2:1 molar ratio) were dissolved in a mixture of chloroform:metanol (2:1, *v/v*). Neutral liposome was prepared by the thin-film hydration method. The chloroform-methanol mixture was evaporated with nitrogen gas to produce a lipid thin film. Incubation was carried out for 1 hr using a vacuum pump to remove residual solvent. Dried films hydrated in 1 mL citric acid buffer (200 mM citric acid, 150 mM NaCl, pH 4.0) and micelle lipid film hydrated HEPES buffer (20 mM HEPES, 150 mM NaCl, pH 7.0) then exactly mixed. In order to make the size of the liposome (100 nm), the liposome solution was serially extruded 10 times by Whatman nuclepore polycarbonate membrane filters (800 nm, 400 nm, 200 nm and 100 nm). After adjusting the size, the liposome solution dissolved in citric acid was buffer changed to pH 7.0 HEPES solution by Dialysis Cassettes. Dialysis is performed at room temperature for 2 hr, the buffer is exchanged, and the buffer is allowed to stand overnight at 4℃. Prepared liposomes and micelles were co-incubated at 60℃ for 1 hr. The doxorubicin was encapsulated in liposomes through the exchange of substances by osmotic pressure. The liposome (1 mg/mL) were reacted with 50 μL (5 mg/mL) doxorubicin at 60℃ for 10 min and vortexed every 2 min. Doxorubicin enters liposomes due to different pH differences inside and outside the liposome. The uncapsulated doxorubicin were separated from liposome by CL-4B gel-filtration (GE Healthcare, Chicago, IL, USA).

Preparation Dual-Apt-Dox

MUC1 and CD44 aptamer (1 nmole) was treated with 10 μL of 100 mM TCEP [tris (2-carboxyethyl) phosphine] for 1 hr at room temperature to destroy disulfide bonds and to generate SH groups and then precipitated ethanol. Next, the aptamer forms a covalent bond with the micelle maleimide group to form an aptamer conjugated micelle in a molar ratio 1:10 for 2 hr at RT. The aptamer conjugated micelle was inserted into the prepared doxorubicin encapsulated liposomes (890 μg) by incubation at 60℃ for 1 hr. Dual-Apt-Dox were purified from free nucleic acids and free micelles by CL-4B gel-filtration. The solution containing dual apatamosome was detected by red fluorescence and concentrated by centrifugation at 3,000 rpm for 30 min using 30 kDa MWCO centricon.

Gel retardation assay

A gel retardation analysis was performed to confirm completion of the dual-aptamosomes. Aptamer (6 pmole) were mixed with the prepared micelle at molar ratio 1:1, 1:5, 1:10 and incubated to complete complexation for 2 hr at RT. After aptamer-micelle complex (1:10) were reacted with liposome at molar ratio 1:2, 1:10 and 1:20. The complexes were loaded on a 1% agarose gel in Tris/borate/EDTA (TBE) buffer and then run at 100 V for 20 min. bands were visualized using.

Competitive binding assay

The Breast cancer stem cells (2×10^4 cells/well) were grown in 24 well plate for 24 hr. After incubation, cells were treated with free Dox, Dual-Apt-Dox, fee aptamer containing an amount of Dox 2 μM in 100 μL of free media and incubation at 37℃ for 40 min. After incubation, cells were gathered by trypsin treatment and collected with 500 μL of PBS. Cells were observed with NovoCyte Flow Cytometer.

Cytotoxicity assay

Cell viability was evaluated by WST assay. MCF-7 cell (3×10^4 cells/well) and Breast cancer stem cell (1.5×10^4 cells/well) were seeded in 96 well plates in 100 μL of 10% FBS-containing EMEM or DMEM/F12 per well. After 24 h incubation, MCF-7 cells and BCSCs were treated with various concentration of Dual-Apt-Dox, Lipo-Dox in 100 μL serum media and the cells were incubated at 37℃ for 48 hr. The cells were treated with 10 μL of EZ-CyTox reagents (Daeil Lab Service, Seoul, South Korea) and after 1 hr of reaction the absorbance was measured at 450 nm using VersaMax ELISA microplate reader. Cells were treated with 10 μL of EZ-CyTox reagent for 1 hr. The absorbance was measured at 450 nm using a VersaMax ELISA microplate reader.

Annexin V/PI staining

Dual-Apt-Dox mediated apoptosis of MCF-7 cells and BCSCs were verified with FITC Annexin V Apoptosis Detection kit (BD Biosciences). MCF-7 cells (9×10^4 cells/well) and BCSC (6×10^4 cells/well) were seeded into 48 well plates. After 24 hr the cells were treated with 2 μM, 4 μM and 8 μM of Dual-Apt-Dox and Lipo-Dox in 200 μL serum free media at 37℃ for 4 hr. The medium was changed with a 10% FBS containing medium and the cells were incubated for an additional at 37℃ for 48 hr. After incubation, the cells were washed twice with PBS buffer and stained with 5 μL of FITC annexin V solution and 5 μL of PI solution in 500 μL of binding buffer for 15 min at RT. Apoptosis of cells were observed with FACS calibur flow cytometer (ACEA Bioscience, San Diego, CA, USA).

Histological analysis

MCF-7 breast cancer stem cells grown in culture were suspended at a density of 6×10^4 cells/200 μL in D5W (5% dextrose DW) and injected into the lateral tail vein of female 8-week-old BALB/c athymic nude mice (n=3 mice per group). Dual-Apt-Dox and Lipo-Dox were administered in the same containing of dox amount of 6 μg in 200 μL of D5W solution and injected into the same mouse with a time interval of one hour. The mice were dissected after 5 weeks.

The lungs and livers were excised and washed with 0.85% NaCl for one day and fixed with 10% formalin. Formalin fixed tissues were washed with water and hydrated with ethanol from 70% to 100%. Then, the tissues were washed twice with xylene and embedded in paraffin. The paraffin embedded tissues were sectioned with 4 μm. The tissues section was deparaffinized and then stained with hematoxylin-eosin (H&E) reagent observed with a light microscope.

Statistical analysis

The experiment results were represented as the means ± SD. Statistical analysis were determined by two-tailed Student's *t*-test method. *$P<0.05$ or **$P<0.01$ were regarded statistically significant.

RESULTS

Expression level of MUC-1 and CD44 antigens in MCF-7 cells and BCSCs

BCSCs were isolated from MCF-7 cells and cultured under non-adherent conditions. Single dissociated BCSCs could regenerate their clonogenicity. Thus, after one week of incubation, the shape of the BCSCs was formed, and the diameter gradually increased for two weeks (Fig. 1A). Before assessing the target delivery of Dual-Apt-Dox, the levels of MUC1 and CD44 proteins in MCF-7 cells and BCSCs were analyzed with a fluorescence microscope (Fig. 1B). Fluorescent images were obtained after the binding of MUC-1 and CD44 DNA aptamers to MCF-7 cells and BCSCs. High fluorescence was each noted in MCF-7 cells treated with the MUC-1 aptamer and in BCSCs treated with CD44 aptamer. These results confirm that MUC-1 and CD44 aptamers are suitable for targeting MCF-7 cells and BCSCs.

Dual-Apt-Dox design and preparation

Breast cancer cells and BSCSs can be targeted by DNA aptamers through membrane-bound specific markers, which can be used for preparing drug delivery vehicles. MUC-1 and CD44 are well-known markers for the targeted delivery of chemotherapeutic agents to breast cancer cells and BCSCs. In this study, MUC-1 and CD44 aptamers were used to prepare targeted liposomes for the delivery of Dox. Fig. 2
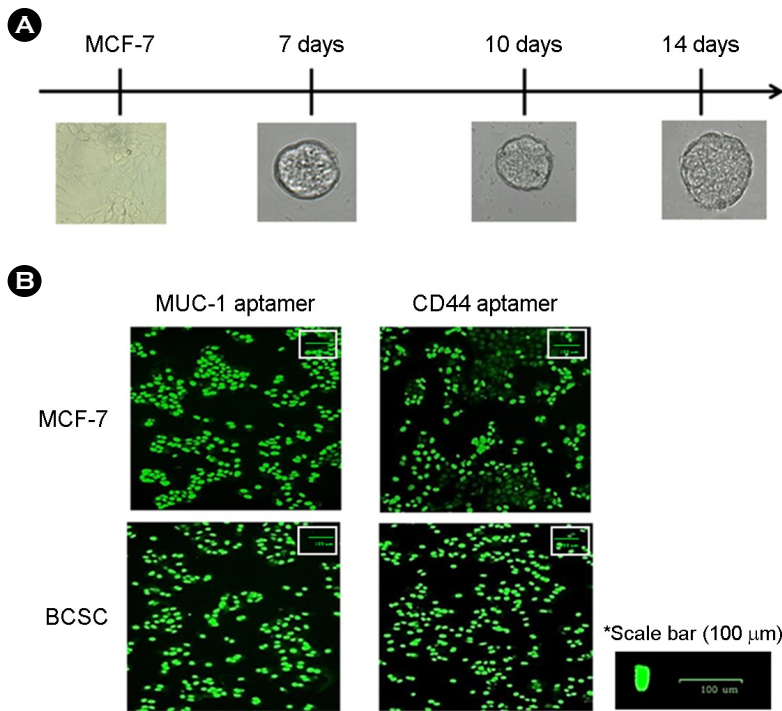
Fig. 1. Morphological change and expression level of MUC-1 and CD44 antigen of MCF-7 cells and BCSCs. (A) Morphology of BCSCs and MCF-7 cells at 7, 10, and 14 days of culture and observed using the microscope. BCSCs and MCF-7 cells were treated with MUC-1 and CD44 aptamer. (B) Cell surface expression levels of CD44 and MUC-1 were green fluorescence in fluorescence microscopy on MCF-7 cells and BCSCs (scale bar=100 μm).

MUC-1 DNA aptamer 5'-FAM-GGC TAT AGC ACA TGG GTA AAA CGA C-SH-3'

CD44 DNA aptamer 5'-FAM-CCA AGG CCT GCA AGG GAA CCA AGG ACA CAG-SH-3'
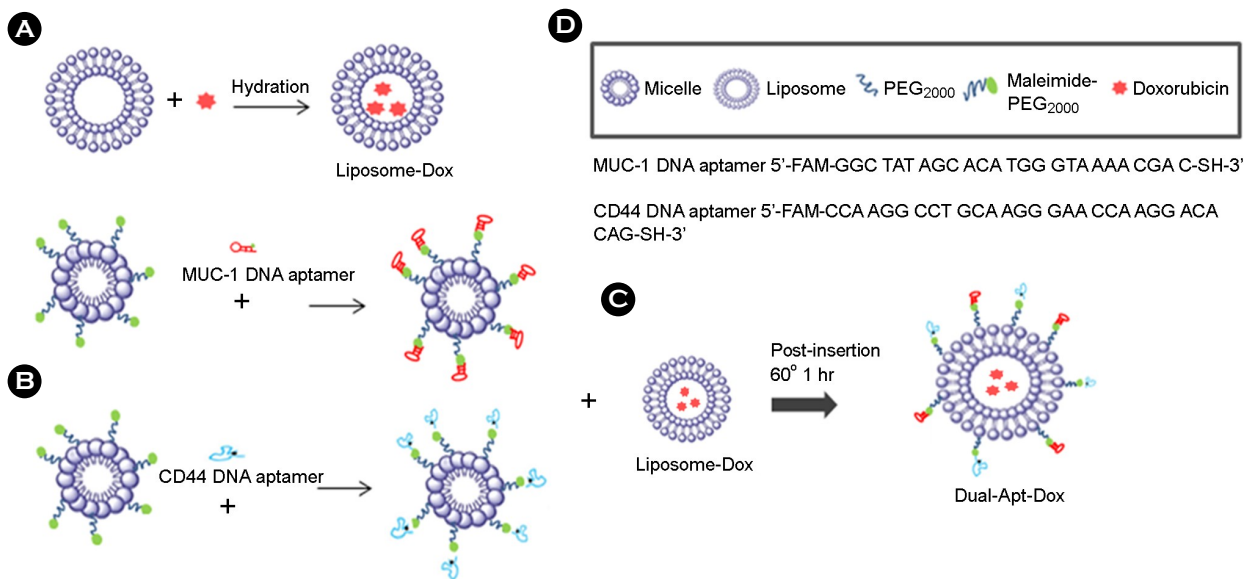
Fig. 2. Schematic diagram of aptamer-linked liposome preparation. (A) Doxorubicin was added to liposomes and captured by proton exchange. (B) The MUC-1/CD44 aptamers were coupled with PEG-Micelles through thiol and maleimide binding reactions. (C) The aptamer conjugated micelles were mixed with a dox encapsulating liposome via the post insertion. (D) Sequence of extended MUC-1 and CD44 DNA aptamer. Linker DNA was modified with FITC and 5'- and 3'-terminal thiols, respectively.

shows a schematic illustration for the preparation of dual-aptamosomes containing Dox. Dox-containing liposomes were prepared in advance, with the capture of Dox being mediated by the pH difference inside and outside the liposomes (pH 7.4 outside and pH 4.0 inside). Dox was loaded into liposomes through proton exchange in and out of the
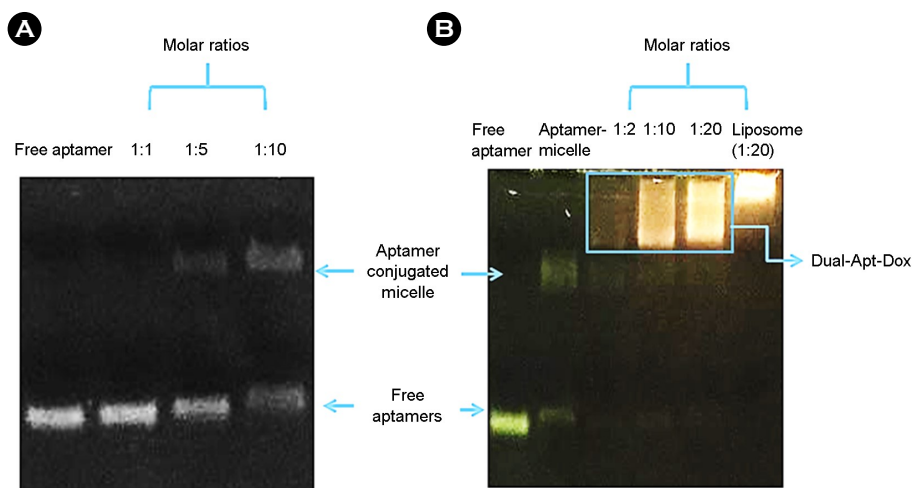
Fig. 3. Gel retardation assay of the aptamer linked liposomes. The optimal ratio of aptamers to micelles and liposomes was determined by gel retardation assay. (A) To find the best ratio of aptamer and micelle, aptamer incubated with aptamer for 1, 5 and 10 molar ratio and 2 hr at room temperature, respectively. (B) To find the optimal ratio of micelle and liposome, aptamer-micelle was reacted with liposomes at various concentrations at 60℃ for 1 hr. Each sample was performed on 1% agarose gel at 100 V for 20 min and observed by UV illumination.

liposomes due to this pH difference (Fig. 2A). MUC-1 and CD44 aptamers were synthesized with PEGylated DSPE (1,2-distearoyl-sn-glycero-3-phosphoethanolamine) micelles using thiol maleimide. The reducing agent TCEP was used to cleave the aptamer-S-S bond to generate an aptamer-SH bond (Fig. 2B). Dox-encapsulated liposomes and aptamer-conjugated micelles were co-incubated at 60℃ for 1 h (Fig. 2C). Fig. 2D describes a sequence of aptamers modified with thiols at the 5'- and 3'-ends. Through this process, liposomes were conjugated with MUC-1 and CD44 aptamers for the targeted delivery of chemotherapeutic agents to breast cancer cells and BCSCs (Dual-Apt-Dox).

Characterization of dual-aptamosomes

A gel retardation assay was performed to determine the optimal ratio of DSPE-PEG$_{2000}$-MUC-1/CD44 aptamer conjugates for the coupling of aptamers and liposomes. Fluorescence density was measured using a chemiluminescence analyzer (Fig. 3). Aptamers and micelles were mixed at 1:1, 1:5, and 1:10 molar ratios and run on a 1% agarose gel. Fig. 3A shows that the combined signal densities of aptamers and micelles were not detected at the molar ratio of 1:1, but a combined signal between aptamers and micelles could be observed at the molar ratio of 1:5. The largest binding signal was identified at a 1:10 molar ratio. Therefore, aptamer-micelles at a molar ratio of 1:10 were used in this study. Next, aptamer-micelles and liposomes were mixed at 1:2, 1:10, and 1:20 molar ratios and run on a 1% agarose gel (Fig.

3B). The last lane was present as a control group, indicating the position of the liposome. The liposome bands at 1:2, 1:10, and 1:20 molar ratios combined with the aptamer-micelles, and the positions of the bands were shifted. Aptamosomes at 1:20 molar ratio was used in this study.

***In vitro* cytotoxicity of Dual-Apt-Dox in MCF-7 cells and BCSCs**

To compare the anticancer effects of Lipo-Dox (non-targeted liposomes encapsulating Dox) and Dual-Apt-Dox, we performed a WST assay on MCF-7 cells and BCSCs. Fig. 4A shows that Dual-Apt-Dox exerts a greater cytotoxic effect, which targets both CD44 and MUC-1. MCF-7 cells treated with Dual-Apt-Dox [8 μM] showed significantly reduced cell viability [(43.7±3.8)%, *$P < 0.05$], while the cells treated with Lipo-Dox [8 μM] exhibited a relatively higher cell viability [(60.3±2.5)%, *$P < 0.05$] than the Dual-Apt-Dox [8 μM]. Fig. 4B shows that Dual-Apt-Dox, which can perform dual targeting, exhibits a more enhanced growth inhibitory effect. Breast cancer stem cells (BCSCs) treated with Dual-Apt-Dox [14 μM] showed significantly reduced cell viability [(46.7±3.5)%, **$P < 0.01$], while the cells treated with Lipo-Dox [14 μM] exhibited a relatively higher cell viability [(85.2±3.7)%, **$P < 0.01$] than the Dual-Apt-Dox [14 μM]. The results showed the increased uptake of Dual-Apt-Dox in MCF-7 cells and BCSCs. Moreover, these results demonstrated that Dual-Apt-Dox is more efficient at inhibiting cell proliferation than the control group.
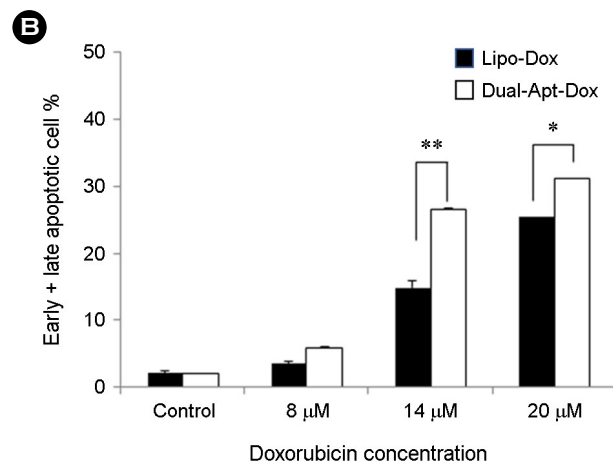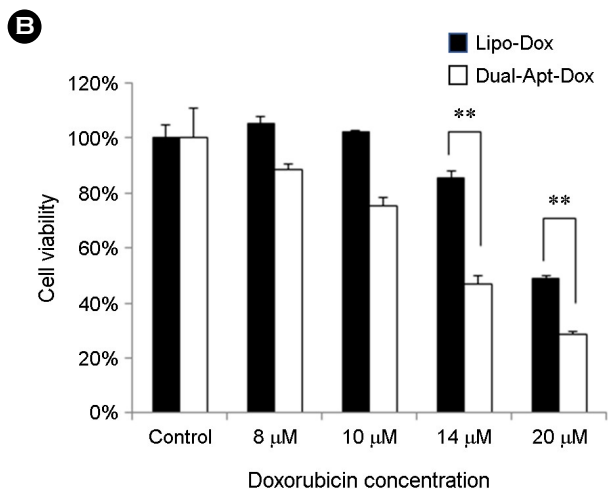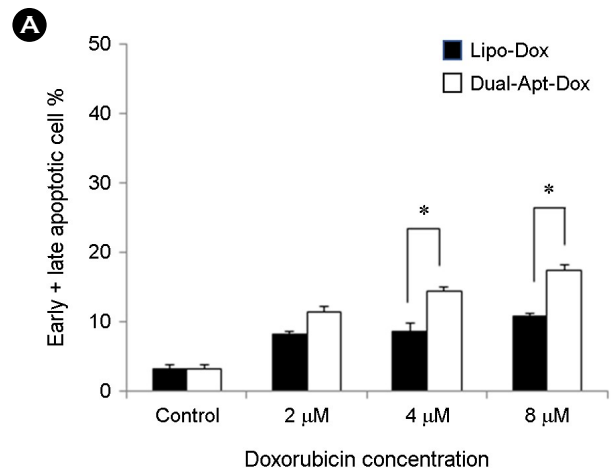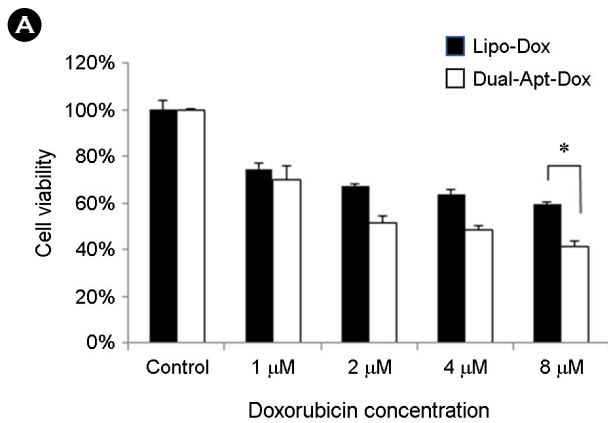
Fig. 4. Cytotoxic effect of Dual-Apt-Dox on MCF-7 cells and BCSCs. (A) MCF-7 cells were treated with Dual-Apt-Dox and Lipo-Dox at varied concentrations of doxorubicin (1, 2, 4, and 8 μM) and (B) BCSCs were incubated with Dual-Apt-Dox and Lipo-Dox (8, 10, 14, and 20 μM) for 48 hr. The survival rate of the treated cells was measured by WST assay. Data shown represent the mean ± SD of three experiments. (*P < 0.05 and **P < 0.01 compared to Dual-Apt-Dox with Lipo-Dox, n=3).

Fig. 5. Induction of apoptosis by dual-apt-dox in MCF-7 cells and BCSCs. Apoptosis assay was performed using flow cytometry to evaluate cell killing effect by apoptosis. (A) MCF-7 was treated with various concentrations of Dual-Apt-Dox and Lipo-Dox (2, 4, 8 μM) at 37℃ for 48 hr. (B) BCSC was incubated with various concentrations of Dual-Apt-Dox and Lipo-Dox (8, 14, 20 μM) at 37℃ for 48 hr. Each bar charts showed quantitative data of average of 3 independent flow cytometry experiments for apoptosis on MCF-7 or BCSCs. Data shown represent the mean ± SD of three experiments. (*P < 0.05 and **P < 0.01 compared to Dual-Apt-Dox with Lipo-Dox, n=3).

Induction of apoptosis by Dual-Apt-Dox in MCF-7 cells and BCSCs

Annexin V-FITC/PI staining was performed to confirm apoptosis induction and the therapeutic effects of Dual-Apt-Dox (Fig. 5). As shown in Fig. 5A, the percentage of apoptotic cells in MCF7 cells treated with Lipo-Dox [8 μM] and Dual-Apt-Dox [8 μM] for 48 h, was 11.8±1.8% and 17.2±2.1%, respectively (*P < 0.05). As shown in Fig. 5B, the percentage of apoptotic cells in drug-resistant BCSCs treated with Lipo-Dox [14 μM] and Dual-Apt-Dox [14 μM]

for 48 h, was 15.8±2.7% and 27.2±1.3%, respectively (**P < 0.01). The results demonstrated that the proportion of early and late apoptotic cells increased with increasing concentrations of Dual-Apt-Dox, which was significantly higher than that of Lipo-Dox. These results indicated that Dox induced apoptotic cell death in MCF-7 cells and BCSCs, and active targeting with Dual-Apt-Dox enhanced cell death.
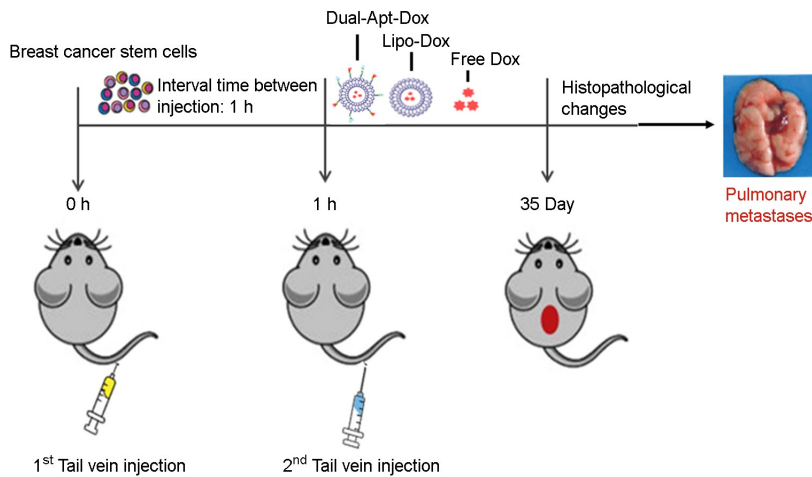
Fig. 6. Schematic diagram of design of the experimental metastasis model. The experiment was designed to confirm the inhibition of BCSC metastasis via Dual-Apt-Dox *in vivo*. BCSCs were prepared before injection in nude mouse. BCSC cells (6×10^4 cells per mouse) were implanted by the lateral tail vein. And then Dual-Apt-Dox were injected into the tail vein of the first injected mouse. After 35 days, metastatic organ were harvested and analyzed by lung tissue staining.
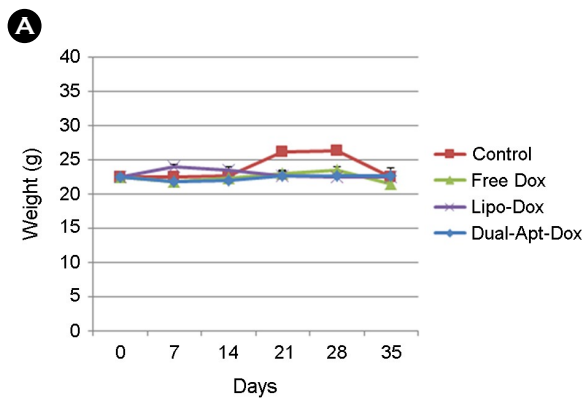

Fig. 7. Pathological changes of lung organs in BCSC metastasis model treated with Dual-Apt-Dox. The mice lung organs were resected on 35th day after tail vein injection of saline, free Dox, Lipo-Dox, Dual-Apt-Dox. (A) Body weight of mice were measured during an experimental period of 35 days (n=4 per group). (B) Paraffin-embedded sections of mice lungs were stained with hematoxylin and eosin (H&E) and observed with a light microscope (Scale bar, 20X: 100 μm, 40X: 50 μm). Mice treated with BCSC alone were used as a negative control, and mice treated only with saline were used as the positive control. The tissues in red dotted lines are pulmonary metastasis regions.
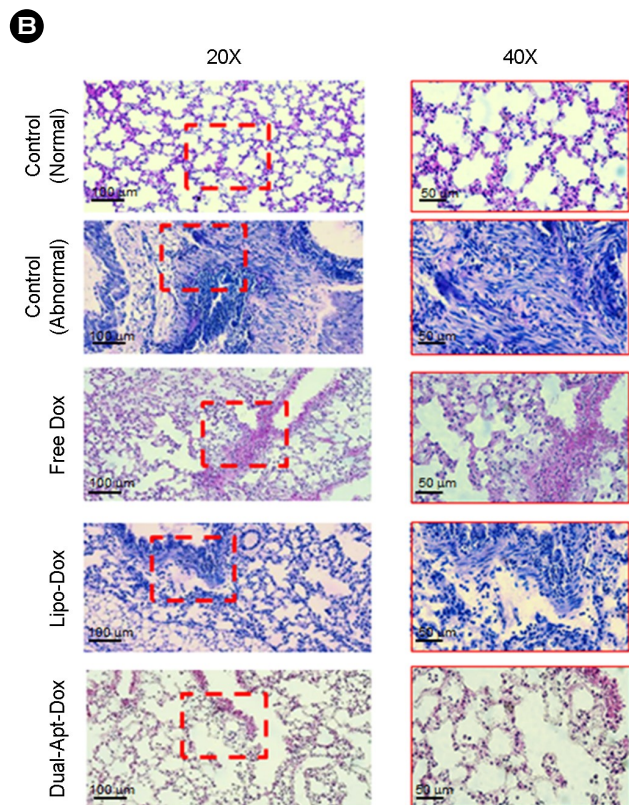
Experimental scheme with a BCSC metastasis mouse model

To examine histopathological changes in BCSC-metastatic mice after treatment with various formulations of Dox, lungs were dissected from the BCSC-transferred mice. First, BCSCs were injected through the lateral tail vein of athymic nude mice. Then, Dual-Apt-Dox, Lipo-Dox, and Free Dox containing 6 μg/mouse of Dox were administered to mice receiving BCSCs at 1 h intervals. The lungs were dissected from the BCSC-metastatic mice on day 35 post-injection (Fig. 6).

Inhibition of metastasis by Dual-Apt-Dox in an *in vivo* model of BCSC metastasis

To evaluate the toxicity of various Dox formulations, the body weights of the mice were monitored for 5 weeks after an intravenous administration of saline, free Dox, Lipo-Dox, and Dual-Apt-Dox (Fig. 7A). Mice treated with Lipo-Dox and Dual-Apt-Dox did not show a significant change in body weight (23.2 g$\pm$1.4% and 23.5$\pm$1.2%, respectively), similar to saline-treated control mice. On the other hand, mice treated with free Dox displayed gradual weight loss over the same period. This result indicated that the liposome nanocarrier did not cause toxicity in mice and reduced the toxicity of the free drug, thereby preventing its side effects on normal tissues. The paraffin-embedded tissue sections of the lungs were stained with hematoxylin and eosin (Fig. 7B). According to microscopic observations of the tissue sections, a certain hypercellular characteristic was observed in the tumor sections of mice treated with Lipo-Dox and free Dox, compared with the negative and positive controls. On the other hand, the tissue sections of the mice treated with Dual-Apt-Dox did not exhibit any serious histological abnormalities, such as inflammation, edema, signet ring, and infiltration. This *in vivo* result suggests that specific nanocarriers for targeted breast cancer cells and BCSCs can effectively deliver anticancer agents and inhibit the metastasis of breast tumors.

DISCUSSION

Currently, cancer recurrence and metastasis due to drug resistance are a major challenge in cancer treatment, which is believed to be caused by CSCs (Minn et al., 2005). Cancer stem cells, which are a small population of cancer cells, have other characteristics that distinguish them from cancer cells; 1) CSCs are well developed with ABC transport pumps, which increase drug resistance by blocking the accumulation of toxic substances in cells, 2) Unlike other cells, CSCs are often in a resting state during the cell cycle. The quiescent state of CSCs is an important anti-proliferative factor and is significantly associated with CSC drug resistance to conventional therapy (Dalerba et al., 2007). Thus, metastatic cancer

spreads more quickly and is resistant to common treatments. Understanding the characteristics of CSCs is important to develop new strategies for the complete treatment of cancer and CSCs. The current challenge is to develop a new platform that can effectively treat cancer by overcoming the drug resistance of cancer and facilitating the accumulation of anticancer drugs at specific tumor sites. The use of nanocarriers for drug delivery presents an optimal cell-friendly solution to reduce drug toxicity (Lin et al., 2012a). Among nanocarriers, liposomes are actively used as carriers for the delivery of antitumor drugs, gene therapeutics, and vaccines (Guan et al., 2018). In our previous study, we developed cholesterol-POPC-based liposome formulae that showed enhanced cellular uptake and release of drugs in the target cells, while reducing the side effects of drugs. POPC, which has a glycerol backbone as a major component of the cell membrane, has the advantage of being cell-friendly and has been used to prepare targeted liposomes because of its neutral charge (Torchilin, 2005). Cholesterol is added to increase the stability of the structure between the liposomes and to improve the stiffness of the lipid layer (Group, 2002). In addition, the CHOL-POPC liposome surface was compounded with PEG. PEG coating on the liposomal surface can increase the intravenous circulation time of the liposome by avoiding the rapid uptake of liposomes by the mononuclear phagocyte system (MPS) and increasing the stability of the liposomal structure. A drug release test of Dox in PBS (pH 7.5) and sodium citrate buffer (pH 4.6) was conducted to evaluate the structural safety of the liposomes (data not shown). The drug release from the liposomes was not significant at pH 7.6, and the liposomes were stable at pH concentrations similar to those in the bloodstream due to the structural safety of the liposomal formulation. However, Dox was rapidly released at pH 4.6, which is similar to the pH of the late endosomes of cells. Therefore, these results indicate that CHOL-POPC liposomes are more effectively internalized by endocytosis. Thereafter, the anticancer drug that enters the cell can rapidly escape from endosomes to exert anticancer effects on tumor cells.

However, the utility of such liposomes has been questioned for the targeting of specific cancer cells. Active targeting liposomes have been considered for the specific targeting

of cancer cells as these use ligands such as antibodies or aptamers that recognize specific proteins expressed by cancer cells (Bazak et al., 2015). Aptamers are easy to use for diagnosis and treatment because they have the advantage of being resistant to heat and chemical denaturation. In addition, aptamers are safe to use *in vivo* because of the less risk of immune rejection that is common in conventional protein-based therapeutics. An aptamer is also considered a synthetic antibody because of its high affinity for the relevant target and its ability to bind to the target (Li et al., 2017). Therefore, in this study, Dox was used to treat cancer cells and CSCs, and the drug was delivered by capturing Dox inside liposomes. Liposomes were conjugated with a dual-aptamer for co-targeting and named Dual-Apt-Dox. For the dual-aptamer system, MUC-1 and CD44 were used as surface markers for MCF-7 and BCSCs, respectively. The optimal ratio of aptamer-conjugated liposomes was determined by gel-retardation assay (Fig. 3). In the cytotoxicity study of MCF-7 cells, the anticancer effect was higher in Dual-Apt-Dox-treated cells (Fig. 4A). These results confirm that cellular targeting of Dual-Apt-Dox improves its interaction with the membrane of MCF-7 cells and facilitates the accumulation of the drug inside the cells. In the cytotoxic effect of BCSCs, when compared to MCF-7 cells, drug resistance was confirmed. Therefore, our study presents a novel strategy to effectively kill drug resistant BCSCs. The results of our study demonstrated that Dual-Apt-Dox significantly suppressed breast cancer by targeting BCSCs. These results confirm that Dual-Apt-Dox inhibits the growth of drug-resistant BCSCs through tumor cell targeting and enhances the sensitivity of BCSCs to anticancer agents.

We have previously reported significant therapeutic potential by using *in vivo* drug-encapsulated aptamosomes to show potent inhibition of tumor growth as well as drug accumulation at the target of the tumor site (Kim et al., 2018). Based on our premise that drug-encapsulated liposomes with double aptamers inhibit CSCs *in vivo*, thus inhibiting the progression of tumors to metastatic state, we evaluated that the inhibition of Dual-Apt-Dox on the metastasis of breast cancer cells and their CSCs (Fig. 7). Importantly, the group treated with Dual-Apt-Dox showed little tumor infiltration similar to that of normal lung tissue. Accordingly, these data suggest that Dual-Apt-Dox can inhibit the metastatic progression of breast tumor through its targeted delivery of anticancer reagents to breast cancer cells as well as CSCs *in vivo*.

In summary, to develop therapeutic nanoparticles targeting breast cancer cells and BCSCs, MUC-1 and CD44-specific DNA aptamers were conjugated to Dox-encapsulated liposomes. These dual-aptamer-conjugated liposomes (Dual-Apt-Dox) showed enhanced anticancer effects on MUC-1/CD44-positive BCSCs as well as cancer cells *in vitro*. In addition, the therapeutic efficacy of Dual-Apt-Dox *in vivo* was demonstrated by inhibiting BCSC-mediated metastasis in mice. Therefore, we propose that aptamer-conjugated liposomes targeting both cancer cells and CSCs can serve as effective therapeutic agents, significantly improving drug treatment efficacy against drug-resistant cancer stem cells.

CONFLICT OF INTEREST

The authors have declared no conflict of interest.

REFERENCES

Bayrac AT, Sefah K, Parekh P, Bayrac C, Gulbakan B, Oktem HA, Tan W. *In vitro* selection of DNA aptamers to glioblastoma multiforme. ACS Chemical Neuroscience. 2011. 2: 175-181.

Bazak R, Houri M, El Achy S, Kamel S, Refaat T. Cancer active targeting by nanoparticles: A comprehensive review of literature. Journal of Cancer Research and Clinical Oncology. 2015. 141: 769-784.

Comşa Ş, Cimpean AM, Raica M. The story of mcf-7 breast cancer cell line: 40 years of experience in research. Anticancer Research. 2015. 35: 3147-3154.

Crabtree JS, Miele L. Breast cancer stem cells. Biomedicines. 2018. 6: 77.

Dalerba P, Cho RW, Clarke MF. Cancer stem cells: Models and

concepts. Annu Rev Med. 2007. 58: 267-284.

Fan C, Georgiou KR, Morris HA, McKinnon RA, Keefe DM, Howe PR, Xian CJ. Combination breast cancer chemotherapy with doxorubicin and cyclophosphamide damages bone and bone marrow in a female rat model. Breast Cancer Research and Treatment. 2017. 165: 41-51.

Ghannam MM, El Gebaly R, Fadel M. Targeting doxorubicin encapsulated in stealth liposomes to solid tumors by non thermal diode laser. Lipids in Health and Disease. 2016. 15: 1-8.

Group ES. Preclinical and phase 1a clinical evaluation of an anti-vegf pegylated aptamer (eye001) for the treatment of exudative age-related macular degeneration. Retina. 2002. 22: 143-152.

Guan J, Shen Q, Zhang Z, Jiang Z, Yang Y, Lou M, Qian J, Lu W, Zhan C. Enhanced immunocompatibility of ligand-targeted liposomes by attenuating natural igm absorption. Nature Communications. 2018. 9: 1-11.

Khodabandehloo H, Zahednasab H, Hafez AA. Nanocarriers usage for drug delivery in cancer therapy. Iranian Journal of Cancer Prevention. 2016. 9.

Kim M, Kim DM, Kim KS, Jung W, Kim DE. Applications of cancer cell-specific aptamers in targeted delivery of anticancer therapeutic agents. Molecules. 2018. 23: 830.

Li J, Wang X, Zhang T, Wang C, Huang Z, Luo X, Deng Y. A review on phospholipids and their main applications in drug delivery systems. Asian Journal of Pharmaceutical Sciences. 2015. 10: 81-98.

Li R, Zheng K, Yuan C, Chen Z, Huang M. Be active or not: The relative contribution of active and passive tumor targeting of nanomaterials. Nanotheranostics. 2017. 1: 346.

Lin X, Gao R, Zhang Y, Qi N, Zhang Y, Zhang K, He H, Tang X. Lipid nanoparticles for chemotherapeutic applications: Strategies to improve anticancer efficacy. Expert Opinion on Drug Delivery. 2012a. 9: 767-781.

Lin Y, Zhong Y, Guan H, Zhang X, Sun Q. Cd44+/cd24-phenotype contributes to malignant relapse following surgical resection and chemotherapy in patients with invasive ductal carcinoma. Journal of Experimental & Clinical Cancer Research. 2012b. 31: 59.

Minn AJ, Kang Y, Serganova I, Gupta GP, Giri DD, Doubrovin M, Ponomarev V, Gerald WL, Blasberg R, Massagué J. Distinct organ-specific metastatic potential of individual breast cancer cells and primary tumors. The Journal of Clinical Investigation. 2005. 115: 44-55.

Pasut G, Paolino D, Celia C, Mero A, Joseph AS, Wolfram J, Cosco D, Schiavon O, Shen H, Fresta M. Polyethylene glycol (peg)-dendron phospholipids as innovative constructs for the preparation of super stealth liposomes for anticancer therapy. Journal of Controlled Release. 2015. 199: 106-113.

Patra JK, Das G, Fraceto LF, Campos EVR, del Pilar Rodriguez-Torres M, Acosta-Torres LS, Diaz-Torres LA, Grillo R, Swamy MK, Sharma S. Nano based drug delivery systems: Recent developments and future prospects. Journal of Nanobiotechnology. 2018. 16: 71.

Saw PE, Park J, Lee E, Ahn S, Lee J, Kim H, Kim J, Choi M, Farokhzad OC, Jon S. Effect of peg pairing on the efficiency of cancer-targeting liposomes. Theranostics. 2015. 5: 746.

Sheridan C, Kishimoto H, Fuchs RK, Mehrotra S, Bhat-Nakshatri P, Turner CH, Goulet R, Badve S, Nakshatri H. Cd44+/cd24-breast cancer cells exhibit enhanced invasive properties: An early step necessary for metastasis. Breast Cancer Research. 2006. 8: 1-13.

Siegel RL, Miller KD, Jemal A. Cancer statistics, 2016. CA: a Cancer Journal for Clinicians. 2016. 66: 7-30.

Sin WC, Lim CL. Breast cancer stem cells—from origins to targeted therapy. Stem Cell Investigation. 2017. 4.

Torchilin VP. Recent advances with liposomes as pharmaceutical carriers. Nature Reviews Drug Discovery. 2005. 4: 145-160.

Trebunova M, Laputkova G, Slaba E, Lacjakova K, Verebova A. Effects of docetaxel, doxorubicin and cyclophosphamide on human breast cancer cell line mcf-7. Anticancer Research. 2012. 32: 2849-2854.

Xing H, Hwang K, Lu Y. Recent developments of liposomes as nanocarriers for theranostic applications. Theranostics. 2016. 6: 1336.

Yan C, Luo L, Guo CY, Goto S, Urata Y, Shao JH, Li TS. Doxorubicin-induced mitophagy contributes to drug resistance in cancer stem cells from hct8 human colorectal cancer cells. Cancer Letters. 2017. 388: 34-42.

Yi SY, Ahn JS, Uhm JE, Lim DH, Ji SH, Jun HJ, Kim KH, Chang MH, Park MJ, Cho EY. Favorable response to doxorubicin combination chemotherapy does not yield good clinical outcome in patients with metastatic breast cancer with triple-negative phenotype. BMC Cancer. 2010. 10: 527.